July 29, 2011

Effect of orbital symmetry of the tip on scanning tunneling spectra of $Bi_2Sr_2CaCu_2O_8+\delta$

Ilpo Suominen
Tampere University of Technology

Jouko Nieminen
Tampere University of Technology

R. S. Markiewicz
Northeastern University

A. Bansil
Northeastern University

Effect of orbital symmetry of the tip on scanning tunneling spectra of $Bi_2Sr_2CaCu_2O_{8+\delta}$

Ilpo Suominen
Department of Physics, Tampere University of Technology, P.O. Box 692, FIN-33101 Tampere, Finland

Jouko Nieminen*
Department of Physics, Tampere University of Technology, P.O. Box 692, FIN-33101 Tampere, Finland and Department of Physics, Northeastern University, Boston

R. S. Markiewicz and A. Bansil
Department of Physics, Northeastern University, Boston
(Received 22 February 2011; published 29 July 2011)

We discuss how variations in the scanning tunneling microscope (STM) tip, whether unintentional or intentional, can lead to changes in topographic images and dI/dV spectra. We consider the possibility of utilizing functionalized tips in order to improve the sensitivity of STM experiments to local irregularities at the surface or hidden below the surface layers. The change in the tip symmetry can radically alter the contrast of the topographic image due to changes in tip-surface overlap. The dI/dV curves change their shape according to which sample bands the tip orbital tends to overlap. In addition, relative phases between competing tunneling channels can be inverted by changing the tip symmetry, which could help reveal the origin of a local irregularity in the tunneling spectrum.

DOI: 10.1103/PhysRevB.84.014528 PACS number(s): 68.37.Ef, 71.20.−b, 74.50.+r, 74.72.−h

I. INTRODUCTION

Scanning tunneling microscopy and spectroscopy (STM/STS) are extensively used to probe the quasiparticle spectra of high-temperature superconductors, especially of the cuprate materials such as $Bi_2Sr_2CaCu_2O_{8+\delta}$ (Bi2212).[1–5] These studies have contributed immensely in obtaining insight into superconducting and pseudogap phases of these materials owing to the very high spatial and energy resolution of the spectroscopy. The full experimental potential of STM/STS is, however, far from exploited, since the chemical and spatial resolution as well as the directional selectivity could, in principle, be improved by overcoming various challenges related to intrinsic properties of STM.

The first challenge is related to the fact that the signal from superconducting layers is filtered by insulating oxide layers. In addition, the signal does not arrive at the microscope tip directly from the site below the tip but rather through symmetry driven tunneling channels. Hence, experimentally observed spectral features are not only distorted by filtering, but ascertaining their spatial origin becomes harder the deeper within the sample is their source. Another factor to be aware of is that the electronic and geometrical properties of the microscope tip may also affect STM images. In standard interpretation, the tip is assumed symmetric to rotations around the vertical axis ("*s* wave"). The relative bluntness of the tip suggests this assumption and, furthermore, the metallic nature of common tip materials does not favor oriented "dangling" orbitals, and specific effects of tip geometry and electronic structure are usually ignored. However, this interpretation has been challenged by a variety of sophisticated theoretical studies,[6–8] which on the one hand show that the closer the tip is to the surface, the more important the symmetry of tip orbitals is to the STM image, and on the other hand, they indicate that *s*-wave tips might not be able to produce images with atomic resolution. Notably, the relative importance of tip orbitals with different symmetries in the STM signal can be controlled by varying the tip-surface distance, or alternatively, by functionalizing the tip by attaching particular atoms or molecules at the apex of the tip.

In various experimental studies,[9–17] the tip properties have been deliberately modified for better spatial or chemical selectivity by picking up a molecule, e.g., CO, O_2, or N_2, from the surface to the apex of the tip after which the plain tip results have been compared to the results with a functionalized tip. This has proven to improve chemical selectivity in adsorbate on a solid surface system since each surface species responds in an individual way to the change of tip symmetry due to functionalization. Even in the case of relatively complicated molecules, such as pentacene attached to the tip, the contrast of differential conductance maps revealing the geometric shape of molecular orbitals is surprisingly sharpened[15] by the enhanced directionality of the probe-sample overlap due to the dominance of the σ or π type localized orbitals closest to the sample surface. The idea of utilizing a functionalized tip is further encouraged by the fact that the resolution of atomic force microscopy (AFM) studies is enhanced by using CO molecule attached to the metallic tip,[18] although improving the resolution and selectivity in the case of AFM has a different physical basis from STM.

The preceding work on molecular adsorbate systems provides motivation for considering functionalized tips for investigating cuprate materials, where the interesting physics is found at layers not immediately on the surface. We can foresee many uses of functionalized tips in probing these materials. An obvious application would be a more accurate probe for the surface properties. In the case of Bi2212, to date one has mostly observed the Bi atoms of the surface layer in topographic STM images. Information from the oxygen atoms of the surface layer has been difficult to obtain, and hence STM provides limited ability to observe the real symmetry of the surface. A more involved application is related to the dI/dV spectra.

As shown in our previous studies,[19] the spectra are mappings of the electronic structure of the cuprate layer, filtered by the BiO and SrO layers, which sit on top of the cuprate layers. Although the signal can be theoretically resolved into partial signals of different origin, the STS experiment measures a signal combined from different sources and, furthermore, the information from different directions in momentum space is integrated into a single outgoing signal. A possible means of decomposing the STS spectrum experimentally is to measure topographic spectral maps. In practice, real-space and Fourier-transformed maps differentiating electron and hole states have been produced in order to recognize direction-dependent underlying electronic order.[20] A third possible application would be investigation of symmetry properties related to nematicity transitions in the subsurface electronic structure at low values of doping, where the oxygen atoms of CuO_2 layers in different directions appear nonequivalent below the pseudogap transition temperature T^* as shown in Ref. 21.

In fact, functionalized tips may well have been used inadvertently in studies of Bi2212. It has been reported that tip resolution can improve dramatically after use, and it has been suggested that this may be due to the attachment of a Bi atom to the tunneling tip.[22] Here we will explore the effects of tips, which are dominated by a single atomic orbital of varying symmetry. We find that such tips can not only couple with different surface orbitals, but can also affect the interference between tunneling channels from the cuprate layer to the microscope tip. This suggests possibilities for investigating irregularities within the cuprate layers, which are not directly accessible to the STM tip, and thus reveal features invisible to STM/STS experiments with a symmetric tip. In this way, our study advances the understanding of matrix element effects in STM.[23–27]

This paper is organized as follows. Section II briefly describes the model utilized in this study. Section III presents calculations of the effect of tip symmetry on topographical maps, STM corrugations, and dI/dV spectra at various high symmetry sites. In Sec. IV we show how a hidden irregularity within the cuprate layer can be studied by comparing results obtained with different tip symmetries, among other results. Finally, conclusions are given in Sec. V.

II. DESCRIPTION OF THE MODEL

Although the model used is essentially the same as in Ref. 19, we provide an overview here for the sake of completeness. The simulation supercell consists of 8 unit cells that have been rotated 45 degrees as shown in Fig. 1. The unit cell geometry is adapted from Ref. 28. In total there are 120 atoms and 2×464 orbitals accounting for both spins. The topmost 7 layers below the cleavage plane are included, which are in descending order: BiO, SrO, CuO_2, Ca, CuO_2, SrO, and BiO. Depending on the atom type different sets of orbitals are included. For Bi, O, and Ca the orbital set is (s, p_x, p_y, p_z) and for Cu the orbital set is $(4s, d_{3z^2-r^2}, d_{xy}, d_{xz}, d_{yz}, d_{x^2-y^2})$. Sr has a single s orbital. The Green's function is computed in a supercell Brillouin zone at 256 equally distributed **k** points corresponding to $8 \times 256 = 2048$ **k** points in the unit cell.

As shown in Fig. 1, we define the position of Cu (or surface Bi) atoms as top site (T), the position of bonding O atoms of the cuprate layer as bridge site (B), and the position of O(Bi) as the hollow site (H). In this choice of geometry, the p_x and p_y orbitals point along the bond between the neighboring Cu atoms, i.e., in the direction from the top site to the bridge site (T $\rightarrow$ B), whereas the linear combinations $\frac{1}{\sqrt{2}}(p_x \pm p_y)$ point from the top site toward the hollow site (T $\rightarrow$ H). Concerning the oxygen atoms related to the cuprate layer, the *apical oxygen* is at the top site, while the *bonding oxygens* between Cu atoms are at bridge sites.

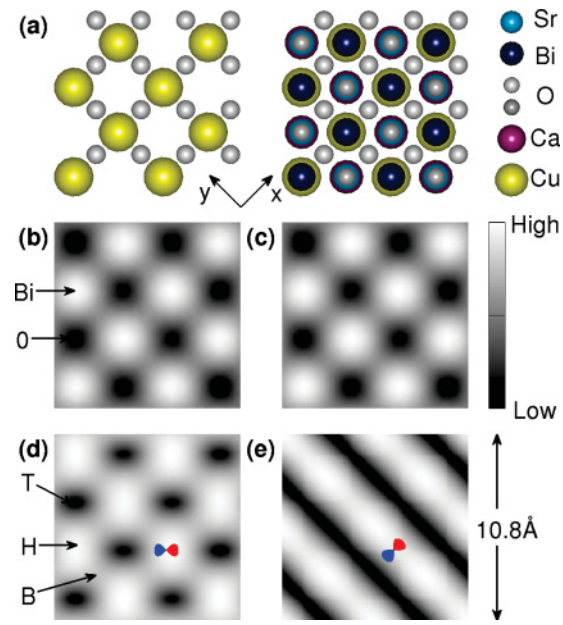

FIG. 1. (Color online) (a) Geometry of the simulated system. Left-hand panel gives the arrangement of the CuO_2 layer, while the right panel depicts the BiO and SrO layers on top of the CuO_2 layer. (b)–(e) Topographic STM images for different tip symmetries. (b) s orbital, (c) p_z orbital, (d) p_r orbital, and (e) p_b orbital. Indicated also are Bi and O positions and the top (T), bridge (B), and hollow (H) sites. In (d) and (e) the tip symmetry is further indicated with a schematic of the corresponding p orbital.

The tip is modeled as a single orbital in order to highlight the effect of each type of tip symmetry on the STM/STS spectrum. We consider four different tip symmetries which can be divided into two groups. These consist of s and p_z orbitals, which are symmetric to rotation around the z axis, accompanied with two choices of horizontal p orbitals. We use a shorthand notation p_b for a p orbital along the bond between two neighboring Cu atoms, and p_r for an orbital rotated by 45°, i.e., aligned in the direction connecting next-nearest neighboring Cu atoms. These two horizontal tip symmetries can also be connected to the nodal (p_r) and antinodal (p_b) directions.

The Hamiltonian is the same as that used previously in our STM studies of optimally doped B2212,[19,29–31] where superconductivity is modeled with a pairing matrix $\Delta_{\alpha\beta}$ between electrons and holes with opposite spins:

$$\hat{H} = \sum_{\alpha\beta\sigma}[\varepsilon_\alpha c^\dagger_{\alpha\sigma} c_{\alpha\sigma} + V_{\alpha\beta} c^\dagger_{\alpha\sigma} c_{\beta\sigma}] + \sum_{\alpha\beta\sigma}[\Delta_{\alpha\beta} c^\dagger_{\alpha\sigma} c^\dagger_{\beta-\sigma} + \Delta^\dagger_{\beta\alpha} c_{\beta-\sigma} c_{\alpha\sigma}], \quad (1)$$

with real-space creation (annihilation) operators $c^{\dagger}_{\alpha\sigma}$ ($c_{\alpha\sigma}$). Indices are a combination of site and spin indices. The d-wave symmetry of the superconducting gap is modeled by taking Δ to be nonzero only between the neighboring $d_{x^2-y^2}$ orbitals, and with opposite signs for x and y directions, which leads to a d-wave symmetric superconducting gap.[32] The tight-binding parameters $V_{\alpha\beta}$ are taken to be doping independent in the spirit of the rigid-band model.[33–35]

The tunneling current is computed within the Todorov-Pendry approximation[36–41] as

$$\sigma = \frac{dI}{dV} = \frac{2\pi e^2}{\hbar}\sum_{tt'ss'}\rho_{tt'}(E_F)V_{t's}\rho_{ss'}(E_F+eV)V^{\dagger}_{s't}. \quad (2)$$

The hopping integrals $V_{\alpha\beta}$ depend on the symmetry of tip and surface orbitals as well as the distances involved through the Slater-Koster coefficients.[42,43] The tip to surface distance is usually greater than the distance between the atoms in the bulk material. To allow for this the standard Slater-Koster method is enhanced by an exponential decay at large distances.[44] The Slater-Koster method allows one to take the directionality of both the tip and surface orbitals into account. It can be considered as a special case of the more general "derivative rule" of Chen[6] and a similar approach of Sacks and Noguera[8] who utilize derivatives of the real-space tip wave function.

There is an alternative way of writing Eq. (2):

$$\sigma = \frac{2\pi e^2}{\hbar}\sum_{tt'cc'}\rho_{tt'}(E_F)M_{t'c}\rho_{cc'}(E_F+eV)M^{\dagger}_{c't}, \quad (3)$$

where

$$M_{tc} = V_{ts}G^{0+}_{sf}V_{fc}. \quad (4)$$

The difference between the two formulas is that Eq. (2) emphasizes the coupling between the tip and the surface orbitals expressed by the hopping integrals V_{ts}, whereas Eq. (3) makes more transparent how tunneling takes place through the filtering layers between the tip and the superconducting layers. Of course the symmetry of the tip itself is described by V_{ts}, but in order to recognize the relevant surface orbitals, it is essential to consider the filtering matrix elements M_{tc} as well.

The spectral function $\rho_{cc'}$ depends on both regular and anomalous Green's functions as shown here:

$$\rho_{cc'} = -\frac{1}{\pi}\sum_{\alpha}(G^{+}_{c\alpha}\Sigma''_{\alpha}G^{-}_{\alpha c'} + F^{+}_{c\alpha}\Sigma''_{\alpha}F^{-}_{\alpha c'}). \quad (5)$$

To conclude, the formulas given above provide not only the total dI/dV spectrum, but also an explicit form of the filtering effect on the cuprate layer, and decompose the density matrix of the cuprate orbitals into regular and anomalous spectral terms.

III. RESULTS

A. Topographic maps

The topographic maps of Figs. 1(b)–1(e) are calculated using Eq. (2) in constant current mode; i.e., there is a feedback loop varying the tip-surface distance in order to retain the tunneling current constant. For bias voltage we choose −0.3 V. We also follow the common practice of accompanying topographic maps with corrugation curves in Fig. 2, since the latter reveal the absolute scale of the contrast otherwise obtained in a rather arbitrary way from topographic maps.

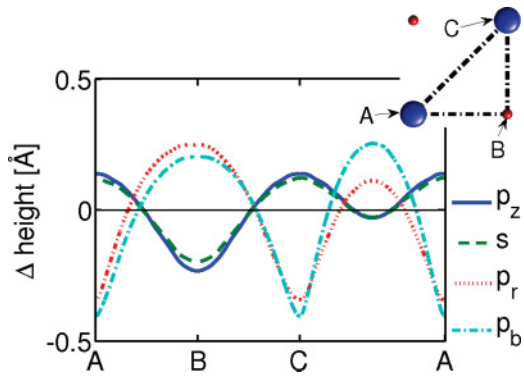

FIG. 2. (Color online) Corrugation curves for various tip orbitals along the route ($A \to B \to C \to A$) shown in the inset. The vertical scale represents the height change the tip experiences along the route. Curves for p_r and p_b are similar in overall shape yet they differ strongly in relative amplitude. This shows that they connect at least partially to different surface orbitals. Note that each curve was shifted downward by its own average tip surface distance thus making all curves zero centered.

Experimental topographic maps typically resemble the calculated maps for an s-wave tip with a high intensity at the position of the surface Bi atoms. Within the Tersoff-Hamann type analysis,[40] a high-intensity signal is attributed to a high local density of electrons. As Fig. 3(a) indicates, the surface Bi atoms have a large density of states over a wide range of energies around the Fermi energy. This was demonstrated already in our earlier work,[19] where we further related this to the coupling between the p_z orbitals of Bi and the d_{z^2} orbital of the Cu atom below through the intermediate p_z orbital of the apical oxygen. In contrast, orbitals of O(Bi) contribute to the BiO bands, which contain a gap around the Fermi energy. In Fig. 3(a) these states are broadened since we have invoked a Fermi liquid type self-energy in the noncuprate layers.[45]

As seen in Figs. 1(b) and 1(c), tips with s as well as p_z symmetry expose the Bi atoms as bright spots. This is hardly surprising, especially in the case of the rather strongly oriented p_z tip orbital. Our computations also suggest that p_z symmetry slightly sharpens the contrast of the topographic map, but as shown in the corrugation curves of Fig. 2, the effect may not be experimentally significant. Tips with in-plane p symmetry show striking changes in topographical maps. In the case where the tip orbital lies along the top-hollow (nodal) direction, p_r [Fig. 1(c)], the contrast is inverted so that O(Bi) atoms appear as bright spots. However, as discussed further in Sec. IV below, visibility of oxygen atoms is spurious since the tunneling signal is still dominated by overlap between the horizontal tip orbital and the p_z orbitals of Bi atoms. This is also the obvious reason why the bright spots in the topographical image lose their sharpness. The change in contrast becomes even more dramatic in the case of the tip orbital lying along the top-bridge (antinodal) direction, p_b. As seen in Fig. 1(d), the fourfold symmetry is now broken, and bright lines appear perpendicular to the orbital direction. In addition, intensity maxima are seen at bridge sites when the bonding oxygen orbital points to the same direction as the tip orbital. This indicates that in this

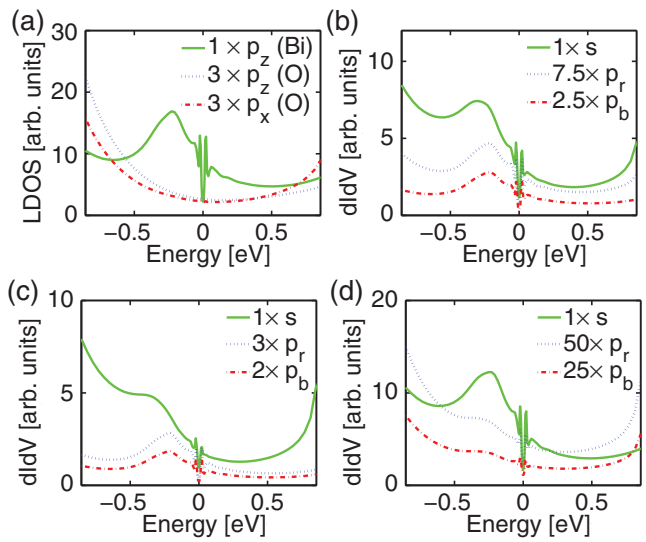

FIG. 3. (Color online) (a) LDOS of p_z of Bi, $p_{x/y}$ of O(Bi), and p_z of O(Bi). The first orbital hybridizes with the CuO_2 bands, the second is dominant in BiO bands (Bi pocket states), and the third is rather localized. (b), (c), and (d) show the dI/dV curves with different tip orbitals at the high-symmetry sites B, H, and T, respectively.

case also the nature of the topographic image is driven by the overlap between the tip orbital and the p_z orbital of Bi atoms.

The intensity patterns in topographic images can be quantified as corrugation curves, such as those shown in Fig. 2. Interestingly, the horizontal tip orbitals not only invert the contrast of the topographic image, but they are also more sensitive to the horizontal position than tips with rotational symmetry around the z axis. This is seen in the more strongly varying corrugation as the tip is scanned between the top, bridge, and hollow sites. These differences, originating from the symmetry-dependent nature of the tip-surface overlap, might be useful in pursuing a better lateral resolution in STM imaging.

Unfortunately, our theoretical predictions cannot be compared directly with measurements at this time since we are not aware of any experimental STM literature on Bi2212 in which a deliberately functionalized tip has been deployed. However, some insight can be obtained by considering a study such as that of Ref. 17, which discusses the effects of attaching O_2 functionalizing molecules to a tungsten tip for investigating a metal phtalocyanine monolayer on an Au(111) surface. Reference 17 finds selectivity with respect to molecular orbitals between normal and O_2-functionalized tips, and observes the STM pattern of the adsorbate monolayer to rotate as different tips are used to probe the surface.

B. dI/dV spectra

The shape and intensity of a dI/dV spectrum depend on the tip symmetry as well as its position. In Figs. 3(b)–3(d), the dI/dV curves are calculated at 5 Å vertical distance between the tip and the surface atoms. At this tip-surface distance, the gap features are clearly observed, and calculations indicate that the signal predominantly comes through the p_z orbitals of the Bi atoms. There are clear changes in the VHS features at ~ -0.15 to -0.4 eV with tip site and orbital symmetry: They seem to vanish for the s-wave tip at a hollow site, and for both the horizontal p-wave tip orbitals at a top site. The apparent reason for this is the increasing spectral weight of the BiO bands with increasing binding energy. These configurations seem to favor a relatively large overlap between the tip orbital and the p orbitals of O(Bi) atoms. For an s-wave tip on the top site, the dI/dV curve resembles the Bi p_z LDOS, as expected. However, this is also true for the horizontal p-wave tips at the bridge or hollow site. These results support the conventional assumption that the experimental tips are predominantly s wave.

We note also a trend in the overall intensities of the spectra. As expected, horizontal p symmetry of the tip orbital tends to decrease spectral intensity due to decreasing overlap. For s-wave symmetry, the intensity is highest for the top site and the lowest for the hollow site. For the horizontal p symmetry, the top site gives the lowest intensity due to antisymmetry between p_z of Bi and the tip orbital. Moving the tip either to the bridge or hollow site allows an increased overlap between the tip orbital and p_z of Bi.

C. Impurity mapping and subsurface irregularities

dI/dV spectra are also used to detect and analyze hidden subsurface irregularities. These can include substitutional impurities, such as Zn or Ni replacing a Cu atom,[3] or dopant atoms like oxygen, the fingerprints of which have been discussed both experimentally[2] and theoretically.[47] However, perhaps the most fascinating potential application may be the $C_4 \rightarrow C_2$ nematic intracell symmetry breaking of the subsurface electronic structure observed at very low values of hole doping in the pseudogap phase.[21] This phase transition in the electronic order is not observed in the topographic images, but rather in dI/dV maps and in the so-called Z maps derived from the differential conductance data. The relevance to the present theoretical considerations arises from the fact that the subsurface bonding oxygen atoms in CuO_2 appear nonequivalent when this low-symmetry phase is mapped. We propose that breaking the symmetry of the tip by functionalization would give additional information about the nematic phase. Note that the observed patterns are difficult to interpret due to the filtering effect of the BiO and SrO layers. It is interesting therefore to explore whether different tip symmetries can provide insight by probing different tunneling channels. In earlier work[19] we showed that the bonding oxygens of the CuO_2 layers are invisible to a spherically symmetric tip placed right above that atom. Hence we choose a local perturbation at this bonding oxygen. The simplest kind of perturbation is a change of the on-site energy, which could be induced by a be nearby dopant atom.

Figure 4(d) shows a tunneling tip positioned above a bonding oxygen in the cuprate layer, equivalent to the bridge site of Fig. 1. To simulate the effect of a nearby impurity, we modify the on-site energy of the p orbital along the bond by -2.0 eV.[48] In Fig. 4(c) we compare its LDOS (blue line) to that of the regular site (red line). The dI/dV spectra from the bridge site with and without on-site modification are plotted for s [Fig. 4(a)] and p_b [Fig. 4(b)] type tips to demonstrate how the impurity effect modifies the spectrum in different tunneling channels. Although the difference between the two

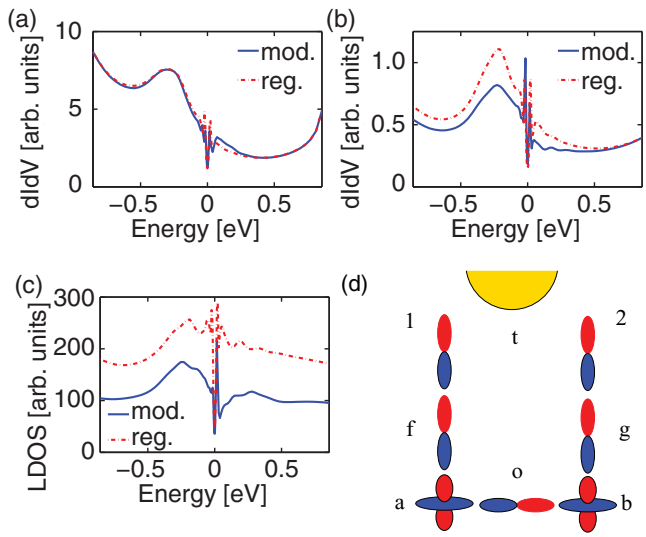

FIG. 4. (Color online) (a) dI/dV spectra of the regular and modified bonding oxygen using s-symmetric tip above the oxygen. (b) The same spectra using p_b-symmetric tip above the oxygen. (c) LDOS of the p orbital of the bonding oxygen in the cuprate layer. *Regular* case (red) is compared with an orbital with a *modified* on-site energy (blue). (d) Two competing channels from the bonding oxygen (o) through d_z orbitals (a or b), apical oxygens (f and g), and the surface bismuths (1 and 2) to the tip (t).

LDOS results is striking [Fig. 4(c)], the spectra obtained by a rotationally symmetric tip do not reflect this difference. This can be explained by the results of Ref. 19, where we showed that two tunneling channels in antiphase are open between the oxygen and the tip [Fig. 4(d)], causing destructive interference between the corresponding signals. (The observed signal comes from different channels involving the Cu atoms.)

In Fig. 4(d) we show the dI/dV curve measured by a tip with p_b orbital, and a clear difference is seen between the spectra of the regular and perturbed oxygens. The shapes of LDOS (b) and the spectra (d) are not identical, but the relative change of the spectrum follows that of LDOS, especially over the range between −0.5 and 0.0 eV. The change in the spectrum of Fig. 4(d) is caused by a reversal of the relative phase between the two tunneling channels in Fig. 4(a) due to p-type symmetry of the tip, a point to which we will return below. This result suggests that experiments probing the breakdown of C_4 symmetry, such as those in Ref. 21, could be further clarified by varying the tip symmetry.

IV. ANALYSIS

A. Tip symmetry and contrast changes in the STM map

A proper understanding of the observed topographical images and spectra requires an analysis of the filtering matrix elements M_{tc} which describe the coupling between the tip and the surface orbitals, propagation across the oxide layers, and coupling between the superconducting cuprate layer and the covering oxide layers. Starting from the latter, the cuprate layer is coupled to the oxide layers mainly through the overlap between the d_{z^2} orbitals of the Cu atoms and the p_z orbitals of the apical oxygen above. The propagation through the oxide layers is mediated by p_z orbitals of the apical oxygen and the Bi atom above on the surface. When the tip symmetry is varied, the relevant factor is that p_z of the surface Bi is the dominant surface orbital mediating the signal from the cuprate layer to the microscope tip. Hence, the analysis of the observed results can be built on the overlap between the tip orbital and the p_z orbitals of the Bi atoms in the vicinity of the tip. While other surface orbitals are present, they are not strongly coupled to the cuprate bands, and hence they have a relatively low spectral weight in the vicinity of the Fermi energy. Thus, the horizontal p orbitals of Bi and O(Bi) atoms are the dominant orbitals of the BiO bands related to the "bismuth pocket" states above Fermi level and the corresponding valence bands below the "spaghetti" of bands [Fig. 3(a)].[49]

Since only the Bi p_z surface orbital is important, the analysis of the various tip orbitals is rather straightforward. The s and p_z orbitals couple best on the top site, as seen in Fig. 3(b). For the horizontal tip orbitals, the overlap between the tip and p_z of a surface Bi is lowest when the tip is directly above the Bi atom. In the case of p_r both the bridge and hollow sites seem to give a large overlap between tip orbital and p_z of Bi, but the hollow sites appear brighter since the overlap between the horizontal p orbitals contributing to BiO bands is larger at this site. For p_b the fourfold symmetry is broken. Since the orbital is oriented along the bonds between Cu atoms, there is a zero-overlap line when following the bonding direction perpendicular to the orbital orientation. On the other hand, p_b overlaps strongly with the two Bi atoms at the bridge site in the antinodal direction of p_b. Moving toward the vicinal hollow sites preserves the strong overlap. At the hollow site, a strong overlap with four Bi atoms can be found. Since the distance is $\sqrt{2}$-fold as compared to the bridge site, overall the overlap remains roughly the same when moving from the bridge site to the hollow site, resulting in bright and dark stripes in Fig. 1(e).

B. Hidden irregularities and the relative phase between two tunneling channels

We consider the possibility of analyzing subsurface irregularities by functionalizing the tip. This may be possible if the interference between two different tunneling channels can be controlled. As an example, let us consider the situation where the tip is at the bridge site [see Fig. 4(d)], i.e., above an oxygen atom in the CuO_2 layer at an equal distance from the two neighboring Bi atoms (1 and 2). This opens two channels from the CuO_2 layer (d_{z2} orbitals of Cu atoms a and b) with filtering matrix elements $M_{1a} = V_{t1} G^0_{1f} V_{fa}$ and $M_{2b} = V_{t2} G^0_{2g} V_{gb}$ which are equally apart from a phase factor. It is obvious that M_{1a} and M_{2b} are equal in the case of an s- or p_z-symmetric tip, since in that case $V_{t1} = V_{t2}$, but the opposite sign is obtained with horizontal p orbitals.

To consider interference effects, we also need to compare elements of the spectral function

$$S_{aoa} = G^+_{ao} \Sigma''_{oo} G^-_{oa},$$
$$S_{bob} = G^+_{bo} \Sigma''_{oo} G^-_{ob},$$
$$S_{aob} = G^+_{ao} \Sigma''_{oo} G^-_{ob},$$

where o denotes the p orbital of the oxygen along the bond between the Cu atoms. It is evident that the p symmetry leads to an antiphase between elements G_{ao} and G_{ob}, and hence the two first spectral terms are equal to each other, but the last one has the opposite sign.

Finally, using Eqs. (3), (4), and (5) we obtain the total current from orbital o to the tip:

$$\begin{aligned} I_o &= \rho_{tt}(|M_{1a}|^2 S_{aoa} + |M_{2b}|^2 S_{bob} + M_{1a} S_{aob} M_{b2}^{\dagger} \\ &\quad + M_{2b} S_{boa} M_{a1}^{\dagger}) \\ &= \rho_{tt}(2|M_{1a}|^2 \mp 2|M_{1a}|^2) S_{aoa}. \end{aligned} \tag{6}$$

It is clear that the "−" sign on the right-hand side of Eq. (6) applies to the case with $V_{t1} = V_{t2}$, i.e., the s or p_z symmetry. Hence the oxygen below the tip would be invisible in STM. On the other hand, constructive interference is obtained for a horizontally p-symmetric tip. This should emphasize any variations in the horizontal p orbital of the bonding oxygen. The situation is of course reversed if the bonding oxygen is replaced by an s-wave symmetric perturbation; i.e., there is a constructive interference for s- and p_z-symmetric tips. This explains our comparison of a spectrum at the bridge site for unperturbed system with a vacancy at the site of the bonding oxygen.

With regard to the $C_4 \rightarrow C_2$ transition, the main practical conclusion of our analysis is that obtaining information related to the nonequivalent bonding oxygens can be enhanced by manipulating the tip symmetry by functionalizing molecules. This suggests that an s-wave symmetric tip gathers the signal from a neighborhood of the bonding oxygen below, while a p-wave tip should be more selective to the on-site oxygen orbitals.

V. CONCLUSIONS

We have investigated the effect of different tip symmetries on topographic STM images and dI/dV spectra. The change in tip symmetry can lead to contrast inversion and even to the breaking up of the C_4 symmetry due to strong differences in the nature of the tip-surface overlap. Furthermore, the corrugation curves show that the horizontal p orbitals at the apex of the tip would be more sensitive to position of the surface atoms. The dI/dV curves reveal the leading sample states (CuO_2-band, BiO-band, or some more localized states) to which different symmetries tend to couple. More strikingly, changing the symmetry of the tip can be used to change the relative phase between two open tunneling channels. This could be applied to detect subsurface irregularities which would otherwise be invisible to STM.

ACKNOWLEDGMENTS

This work is supported by US Department of Energy Grant No. DE-FG02-07ER46352 and benefited from the allocation of supercomputer time at NERSC and Northeastern University's Advanced Scientific Computation Center (ASCC). I.S. would like to thank the Ulla Tuominen Foundation for financial support. This work benefited from the resources of the Institute of Advanced Computing, Tampere. Discussions with Matti Lindroos are gratefully acknowledged.

*jouko.nieminen@tut.fi

[1] Ø. Fischer, M. Kugler, I. Maggio-Aprile, Chr. Berthod, and Chr. Renner, Rev. Mod. Phys. **79**, 353 (2007).
[2] K. McElroy, J. Lee, J. A. Slezak, D.-H. Lee, H. Eisaki, S. Uchida, and J. C. Davis, Science **309**, 1048 (2005).
[3] E. W. Hudson, K. M. Lang, V. Madhavan, S. H. Pan, H. Eisaki, S. Uchida, and J. C. Davis, Nature (London) **411**, 920 (2001).
[4] S. H. Pan, E. W. Hudson, K. M. Lang, H. Eisaki, S. Uchida, and J. C. Davis, Nature (London) **403**, 746 (2000).
[5] A. N. Pasupathy, A. Pushp, K. K. Gomes, C. V. Parker, J. Wen, Z. Xu, G. Gu, S. Ono, Y. Ando, and A. Yazdani, Science **320**, 196 (2008).
[6] C. J. Chen, J. Vac. Sci. Technol. A **6**, 319 (1988); Phys. Rev. Lett. **65**, 448 (1990); Phys. Rev. B **42**, 8841 (1990); Phys. Rev. Lett. **69**, 1656 (1992).
[7] A. N. Chaika, S. S. Nazin, V. N. Semenov, S. I. Bozhko, O. Lübben, S. A. Krasnikov, K. Radican, and I. V. Shvets, Europhys. Lett. **92**, 46003 (2010).
[8] W. Sacks and C. Noguera, Phys. Rev. B **43**, 11612 (1991).
[9] D. M. Eigler, C. P. Lutz, and W. E. Rudge, Nature (London) **352**, 600 (1991).
[10] L. Bartels, G. Meyer, and K.-H. Rieder, Appl. Phys. Lett. **71**, 213 (1997).
[11] L. Bartels, G. Meyer, K. H. Rieder, D. Velic, E. Knoesel, A. Hotzel, M. Wolf, and G. Ertl, Phys. Rev. Lett. **80**, 2004 (1998).
[12] J. R. Hahn and W. Ho, Phys. Rev. Lett. **87**, 196102 (2001).
[13] H. J. Lee and W. Ho, Science **286**, 1719 (1999).
[14] J. Lagoute, K. Kanisawa, and S. Fölsch, Phys. Rev. B **70**, 245415 (2004).
[15] J. Repp, G. Meyer, S. M. Stojkovic, A. Gourdon, and C. Joachim, Phys. Rev. Lett. **94**, 026803 (2005).
[16] Z. T. Deng, H. Lin, W. Ji, L. Gao, X. Lin, Z. H. Cheng, X. B. He, J. L. Lu, D. X. Shi, W. A. Hofer, and H.-J. Gao, Phys. Rev. Lett. **96**, 156102 (2006).
[17] Z. Cheng, S. Du, W. Guo, L. Gao, Z. Deng, N. Jiang, H. Guo, H. Tang, and H. -J. Gao, Nano Research, doi:10.1007/s12274-011-0108-y (2011).
[18] L. Gross, F. Mohn, N. Moll, P. Liljeroth, and G. Meyer, Science **325**, 1110 (2009).
[19] J. Nieminen, I. Suominen, R. S. Markiewicz, H. Lin, and A. Bansil, Phys. Rev. B **80**, 134509 (2009); I. Suominen, J. Nieminen, R. S. Markiewicz, and A. Bansil, *ibid.* **83**, 024501 (2011).
[20] J. Hoffman *et al.*, Science **295**, 466 (2002); D. Zhang and C. S. Ting, Phys. Rev. B **67**, 100506R (2003); Q.-H. Wang and D.-H. Lee, *ibid.* **67**, 020511R (2003).
[21] Y. Kohsaka *et al.*, Science **315**, 1380 (2007).
[22] V. Madhavan (private communication).
[23] Matrix element effects are well known to be important in other highly resolved spectroscopies such as angle-resolved

photoemission (Ref. 24), resonant inelastic x-ray scattering (RIXS) (Ref. 25), Compton scattering (Ref. 26), and positron annihilation (Ref. 27).

[24]S. Sahrakorpi, M. Lindroos, R. S. Markiewicz, and A. Bansil, Phys. Rev. Lett. **95**, 157601 (2005); M. Lindroos and A. Bansil, *ibid*. **77**, 2985 (1996); A. Bansil, M. Lindroos, S. Sahrakorpi, and R. S. Markiewicz, Phys. Rev. B **71**, 012503 (2005); M. C. Asensio, J. Avila, L. Roca, A. Tejeda, G. D. Gu, M. Lindroos, R. S. Markiewicz, and A. Bansil, *ibid*. **67**, 014519 (2003).

[25]R. S. Markiewicz and A. Bansil, Phys. Rev. Lett. **96**, 107005 (2006); Y. W. Li, D. Qian, L. Wray, D. Hsieh, Y. Xia, Y. Kaga, T. Sasagawa, H. Takagi, R. S. Markiewicz, A. Bansil, H. Eisaki, S. Uchida, and M. Z. Hasan, Phys. Rev. B **78**, 073104 (2008).

[26]A. Bansil, R. S. Rao, P. E. Mijnarends, and L. Schwartz, Phys. Rev. B **23**, 3608 (1981); P. E. Mijnarends and A. Bansil, *ibid*. **13**, 2381 (1976); G. Stutz, F. Wohlert, A. Kaprolat, W. Schülke, Y. Sakurai, Y. Tanaka, M. Ito, H. Kawata, N. Shiotani, S. Kaprzyk, and A. Bansil, *ibid*. **60**, 7099 (1999).

[27]P. E. Mijnarends, A. C. Kruseman, A. van Veen, H. Schut, and A. Bansil, J. Phys. Condens. Matter **10**, 10383 (1998); L. C. Smedskjaer, A. Bansil, U. Welp, Y. Fang, and K. G. Bailey, Physica C **192**, 259 (1992).

[28]V. Bellini, F. Manghi, T. Thonhauser, and C. Ambrosch-Draxl, Phys. Rev. B **69**, 184508 (2004).

[29]J. A. Nieminen, H. Lin, R. S. Markiewicz, and A. Bansil, Phys. Rev. Lett. **102**, 037001 (2009).

[30]In the present calculations, we apply a self-energy adapted from Ref. 31 to the $d_{x^2-y^2}$ orbitals of Cu atoms in order to obtain a realistic dispersion renormalization.

[31]Tanmoy Das, R. S. Markiewicz, and A. Bansil, Phys. Rev. B **81**, 174504 (2010).

[32]J.-M. Tang and M. E. Flatté, Phys. Rev. B **66**, 060504(R) (2002); **70**, 140510(R) (2004).

[33]We expect the rigid-band model to be a good approximation for doping away from the CuO_2 planes. It will be interesting to further examine doping effects by using supercell or other first-principles approaches (Refs. 34, 35).

[34]A. Bansil, Z. Naturforsch. A: Phys. Sci. **48**, 165 (1993); H. Asonen, M. Lindroos, M. Pessa, R. Prasad, R. S. Rao, and A. Bansil, Phys. Rev. B **25**, 7075 (1982); R. Prasad and A. Bansil, *ibid*. **21**, 496 (1980).

[35]S. N. Khanna, A. K. Ibrahim, S. W. McKnight, and A. Bansil, Solid State Commun. **55**, 223 (1985); L. Huisman, D. Nicholson, L. Schwartz, and A. Bansil, Phys. Rev. B **24**, 1824 (1981).

[36]T. N. Todorov, G. A. D. Briggs, and A. P. Sutton, J. Phys. Condens. Matter **5**, 2389 (1993).

[37]J. B. Pendry, A. B. Prêtre, and B. C. H. Krutzen, J. Phys. Condens. Matter **3**, 4313 (1991).

[38]This equation can also be derived as a special case of the Landauer-Büttiker approach as expressed in Ref. 39. On the other hand, Eq. (2) can be converted into the Tersoff-Hamann (Ref. 40) formalism in the limiting of a spherical tip orbital in real space (Ref. 41).

[39]Y. Meir and N. S. Wingreen, Phys. Rev. Lett. **68**, 2512 (1992).

[40]J. Tersoff and D. R. Hamann, Phys. Rev. B **31**, 805 (1985).

[41]A. Korventausta, S. Paavilainen, E. Niemi, and J. Nieminen, Surf. Sci. **603**, 437 (2009).

[42]J. C. Slater and G. F. Koster, Phys. Rev. **94**, 1498 (1954).

[43]W. A. Harrison, *Electronic Structure and Properties of Solids* (Dover, New York, 1980).

[44]Note that the density matrices in Eq. (2) concern, in principle, an interacting system. An alternative approach would be to use noninteracting density matrices and replace the hopping terms by a T matrix, $T = V(1 - GV)^{-1}$. However, for the tip distance used in this work, the tip-sample hopping terms are of the order of 0.01–0.02 eV, while the interaction terms within the sample are of the order of 1 eV (e.g., the hopping between p_b of the bonding oxygen and the $d_{x^2-y^2}$ of the neighboring Cu atom is 1.62 eV). Hence, it is safe to utilize noninteracting density matrices in calculating the conductance.

[45]LDA calculations tend to give conducting BiO bands the bottom of which are slightly below Fermi level. However, one never observes these states in ARPES or STS, and hence it is possible that doping the Bi2212 samples may lift these states off the Fermi level (Ref. 46).

[46]H. Lin, S. Sahrakorpi, R. S. Markiewicz, and A. Bansil, Phys. Rev. Lett. **96**, 097001 (2006).

[47]Y. He, T. S. Nunner, P. J. Hirschfeld, and H.-P. Cheng, Phys. Rev. Lett. **96**, 197002 (2006).

[48]We tested several values for the on-site energy, but this value was chosen to best exemplify the effect of a local perturbation at the bonding oxygen site.

[49]p_z of O(Bi) should be rather weakly hybridized with any orbitals; possibly it is very localized and hence gives only marginal contributions to the spectra.